Jurnal Mekanikal
June 2015, Vol 38, 92-105

RELIABILITY ANALYSIS OF THREE POINT BENDING STRENGTH OF POROUS SINTERED CLAY

Muazu Abubakara[1,2], Mohd Nasir Tamin[1], and Norhayati Ahmad[1]*

[1]Faculty of Mechanical Engineering,
Universiti Teknologi Malaysia,
81310 UTM Johor
Johor, Malaysia

[2]Department of Mechanical Engineering,
Bayero University,
Kano, Nigeria

ABSTRACT

In this research, a three parameter Weibull probability distribution was used to model the reliability of the flexural strength of inexpensive porous sintered clay. The as-received clay and the porous sintered clay were characterized by XRF, XRD, BET and FESEM. The clay powders mixed with 10wt% cassava starch were compacted and sintered at a temperature of 1300°C. The flexural strength of the sintered samples (33 samples) was determined by three point bending test. The flexural strength data was analyzed using three-parameter Weibull with Minitab 15 software. Maximum likelihood (ML) and least square (LS) estimates were employed in determining the Weibull parameters. The Weibull modulus value of LS (3.28) was found to be higher than ML (2.21). the Weibull modulus obtained is found to be higher compared to other engineering materials while the threshold strength (11.18-12.97MPa) was lower than other engineering materials. The flexural strength analysis of porous sintered clay shows higher reliability and a three parameter Weibull gives detail reliability of the flexural strength of the porous sintered clay.

Keywords : *Flexural strength, Weibull modulus, threshold, porous clay, reliability analysis.*

1.0 INTRODUCTION

Clay minerals have recently been used as substitute in the production of porous ceramics for filtration application due to the rising cost of engineering ceramics such as oxides, carbides and nitrides. Clay mineral such as kaolin can be an excellent and a cheaper source of mullite ceramic, that is normally prepared from expensive precursors of Al_2O_3 and SiO_2 [1]. Mullite, a major component of aluminosilicate ceramic, shows a good mechanical, chemical and thermal property, low value of coefficient of thermal expansion, low density and good creep resistance [2]. Clay-based ceramic has been used in the fabrication of porous ceramic used in novel areas such as catalyst supports, hot gas or molten metal filters and membranes [3].

*Corresponding author: nhayati@mail.fkm.utm.my

Though, clay-based ceramic membranes have inferior mechanical properties compared with their engineering ceramic counterparts, clay-based membranes for filtration applications have been manufactured by compaction, gelcasting, paste casting and extrusion [4-7]. Compaction has been the cheapest and easiest means of producing ceramic membrane. However, the problem of particle-wall friction hinders the transmission of pressure which resulted in density gradients in the compacts. Clay-based porous membranes have been prepared with a dead-module of diameter 50-55 mm and thickness 5-10 mm by compaction [8-10]. Compacting larger volume ceramic material makes it prone to flaws, which tend to decrease the strength [11]. In addition, there is a tradeoff between permeability and volume when compacting large volume porous ceramic; the higher the volume the less the permeability and vice versa. Therefore, compacting thin membranes will give a porous ceramic with better mechanical and operational properties.

Clay-based membranes have been used for micro and ultrafiltration applications for the treatment of wastewater with a pressure driven membrane process in trans-membrane pressure range 0.07-0.5 MPa and average pore sizes 0.285-4.58 μm and 15 nm [8], [12-15].

Several authors have reported the flexural strength of clay-based ceramic membrane which shows a variation at almost the same sintering temperature (Table 1). Despite the availability of the flexural strength of porous sintered clay [8], [12], [16-17] the reliability of the flexural strength of the porous sintered clay materials have not been well understood, because each study reported a single flexural strength. [18] reported that multiple strength determination of porous materials needed to be conducted, because porous materials under the same fabricating condition may have different porosity, flaws and inclusions which affect connectivity and grain morphology and result in different mechanical property. These variations in the mechanical property data in the ceramic community are evaluated using the Weibull probability distribution. Three-parameter Weibull probability distribution provides detail reliability analysis of the strength than the two-parameter Weibull probability distribution, because the three-parameter Weibull provides the threshold strength below which all the materials will not fail, while the scale parameter in two-parameter Weibull is the strength value at 63.2% [11].

Table 1 Variation of flexural strength of Kaolin-based porous materials together with currently investigated porous material.

Porous Material	Flexural Strength (MPa)	References
Kaolin A	11.55	[4]
Kaolin B	15.54	[8]
Kaolin C	11	[12]
Kaolin D	8	[16]
Kaolin E	7.2	[17]
Kaolin F	13.53-23.26	This research

Currently, there has been a lack of clear understanding of the effects of the stress threshold of clay-based porous ceramics. This can lead to an overestimation of the probability of failure, when we adopt the fitted simple distribution in the prediction of failure and reliability/safety limits of porous ceramic materials produced from traditional clays when they operate under pressure. This study involves the characterization of the clay and the determination of the flexural strength of the porous sintered clay for membrane filtration applications. The flexural strength will be evaluated using three-parameter Weibull

distribution to determine the Weibull modulus and the threshold strength i.e., the strength below which all the clay-based porous ceramics will not fail.

2.0 EXPERIMENTAL PROCEDURE

X-ray diffraction (XRD) analysis and X-ray fluorescence spectroscopy was performed as reported in [19]. The clay mixed with 10%wt cassava starch were compacted after adding drops of glycerol which acted as a binder to dimension 3×80×50 with an INSTRON 600DX. The samples (33 each for the porous ceramic) were sintered for 2 hours at a temperature of 1300°C. The density of the porous ceramic was measured using Archimedes principle and was found to be 21.7%.

BET measurements were carried out on TriStar II 3020 surface area and pore analyzer with N_2 as adsorbate at -196°C for 4 h in a vacuum. The BET surface area was determined with the adsorption branch of isotherm in the P/P_o range 0.05-0.3 based on the conventional Brunauer-Emmett-Teller (BET) equation (S_{BET}) and α_s method from the adsorption data at -196°C. The total pore volume was determined with the amount of nitrogen adsorbed at a relative pressure P/P_o 0.99 and the average pore diameter was calculated from $D= 4V_p/ S_{BET}$. BJH method was employed in the calculation of pore size distribution (PSD).

2.1 Three – Point Bending

The flexural strength of the samples and associated variations is established through series of three-point bending test of the rectangular specimen. The specimen measures 4×80×30mm, with a span length of 40mm. The test was conducted using Instron 100-KN electro-mechanical testing machine, at a loading rate of 0.5mm/min, based on the following equation:

$$\sigma = \frac{3PL}{2bd^2} \tag{1}$$

where P is the load, L is the span which is 40mm, b is the width and d is the thickness. Figure1 shows a selected pattern of the fracture mode of the porous ceramics. From the Figure it can be deduced that all the fractured samples exhibited a brittle mode of failure.

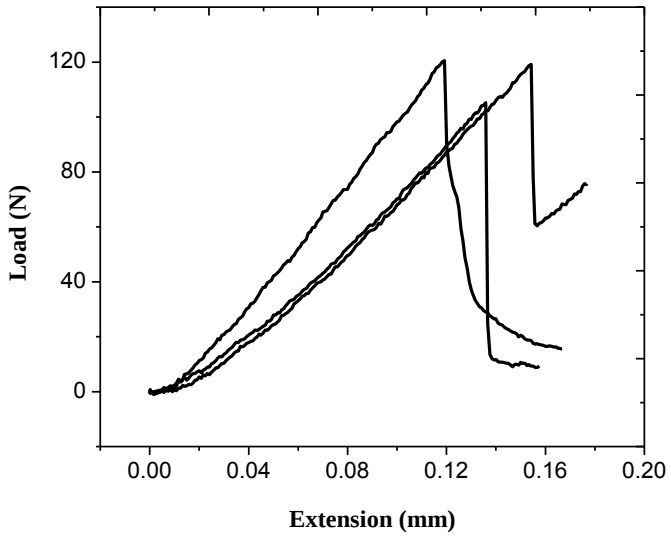

Figure 1 Graphs of load vs extension of porous ceramic.

2.1 Review of Weibull Statistics

The cumulative failure distribution function of the three parameter Weibull probability distribution [20], is given by :

$$P_f = 1 - \exp\left[-\left(\frac{\sigma - \sigma_u}{\sigma_o} \right)^m \right] \tag{2}$$

where P_f is the failure probability for a given flexural strength σ, σ_o is the characteristic strength (scale parameter), the slope $\hat{m}$ is the Weibull modulus (shape parameter); higher $\hat{m}$ means less probability that the material will fail an indication of more even distribution of defects and σ_u is the threshold, i.e., the flexural strength below which the material will not fail. When σ_u=0, the three-prameter Weibull reduces to two-parameter Weibull.

If the reported flexural strength has high uniformity, the threshold strength should not be zero [21] and the data should more appropriately model using the three parameter Weibull. The three parameter Weibull can be solved using linear regression or by maximum likelihood.

In least square estimate Eq 1 is linearized to obtained

$$\ln\left[\ln\left(\frac{1}{1 - P_f} \right) \right] = m\left[\ln(\sigma - \sigma_u) - \ln \sigma_o \right] \tag{3}$$

The maximum likelihood estimation of the three Weibull parameters (σ, σ_u, and σ_o) is expressed by the following log-likelihood function of Eq 4. [22]:

$$\ln L = \sum_{i=1}^{N} \ln\left\{ \frac{m}{\sigma_o} \left(\frac{\sigma - \sigma_u}{\sigma_u} \right)^{m-1} \exp\left[-\left(\frac{\sigma - \sigma_u}{\sigma_o} \right)^m \right] \right\} \tag{4}$$

The solution is found by maximizing the log-likelihood function and solving for $\hat{m}$, $\hat{\sigma}_o$ and $\hat{\sigma}_u$ such that the variation with respect to each Weibull parameter diminishes, i.e., $\delta \ln L/\delta m = 0$, $\delta \ln L/\delta \sigma_0 = 0$, and $\delta \ln L/\delta \sigma_u = 0$ [23]. ML offers some advantages in estimating the Weibull parameters such as consistency, asymptotic normality-convergence of the distribution for infinite number of samples, and asymptotic efficiency-optimality of an estimator [11]. In addition, it is not necessary to use any formula when using ML in determining the plotting positions.

The data were analysed using Minitab 15 software to determine the shape, scale and threshold parameters at 95% CI of the porous ceramic. Various estimates such as mean rank, median rank, Kaplan Meier and modified Kaplan Meier (Hazen rank) were used to determine which estimate best fits the data. The mathematical representations of the formulae are respectively [24] and [25].

$$P_f = \frac{Q_i}{N+1} \tag{5}$$

$$P_f = \frac{Q_i - 0.3}{N + 0.4} \tag{6}$$

$$P_f = \frac{Q_i - 0.5}{N} \tag{7}$$

$$P_f = \frac{Q_i}{N} \tag{8}$$

where Q_i is the ranked flexural strength arranged in ascending order and N is the total number of samples into consideration.

3.0 RESULTS AND DISCUSSION

The chemical composition of the raw clay is found to be 55% SiO_2, 42.9% Al_2O_3, 1.3% K_2O, 0.3% Fe_2O_3, and 0.06% CaO. The XRD analysis of the raw clay and sintered clay at 900-1200°C is shown in Figure 2. The XRD analysis of the raw clay shows that kaolinite is the major phase with traces of illite and quartz. These are the main constituent phases present in kaolin clay [19]. The sintered clay shows diminishing of heated muscovite phase when the clay is sintered from 900-1100°C; at 1200°C, mullite phase formed and becomes pronounced at 1300°C. Mullite formed after sintering temperature of 1100°C with no cristobalite phase; the disappearance of cristobalite phase can be attributed to the heating rate at 10°/min, which is enough to cause the disappearance of the phase [26].

The nitrogen adsorption BET measurement was employed to investigate pore properties of the porous sintered clay. The isotherm of the porous sample is shown in Figure 3 and identified as type IV isotherm according to Branauer's classification with H3 hysteresis; the isotherm presents a step down in the desorption isotherm, which is associated with the hysteresis loop closure, this behavior shows the porous material has a slit shape pores. Pore volume of the porous sample was found to be 0.001264cm^3/g. The BET surface area (S_{BET}) obtained for the porous material is 0.9366m^2/g.

The pore size distribution is shown in Figure 4. From the PSD, the porous material exhibit peaks at 19.98Å, 36.15Å, 44.95Å, with average pore size of 53.964Å, which signifies the porous material, is mesoporous.

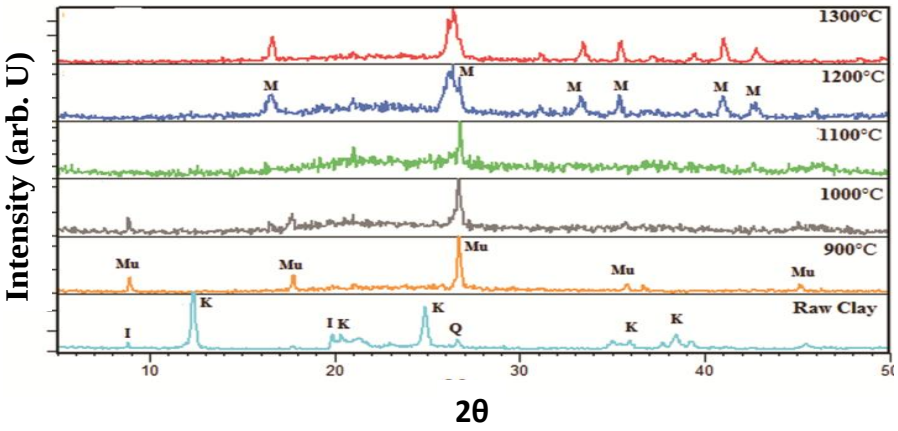

Figure 2 XRD analysis of as-received clay and sintered clay at different temperatures, K= kaolinite, Q= quartz, I= illite, Mu=Muscovite, M= mullite [19].

The adsorption/desorption isotherm gives a slow increase in the adsorption amount of nitrogen at a relative pressure up to 0.9 due to capillary condensation and low slope region in the middle of the isotherm, which indicates the presence of mesopores as reported by [27].

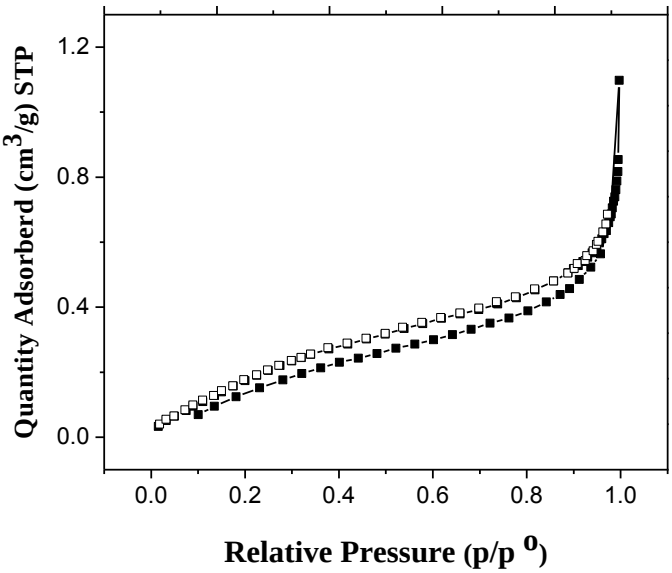

Figure 3: Adsorption/Desorption isotherm of the porous sintered clay.

Then the shape of the isotherm increases sharply at high relative pressure at approximately 1.0 and exhibit hysteresis. The hysteresis formed is an indication of the presence of slit shaped pore, which is common to H3 type hysteresis. An average pore size of 53.9640Å further supported that the material is mesoporous.

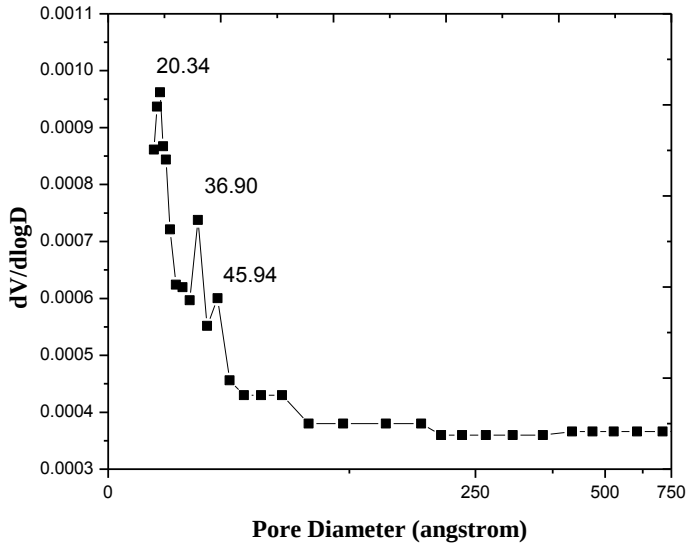

Figure 4: Pore size distribution of the porous sintered clay.

Various statistical distributions were tested for the goodness-of-fit for the porous samples produced using Minitab software. Three parameter Weibull distribution gave the best result for the materials with P-value (0.024), lowest Anderson-Darling statistics (0.583) and near zero likelihood ratio test (LRT-P) value (0.006) for the porous ceramic.

Table 2 shows the summary of the shape, scale, threshold and Anderson-Darling statistics value for least square and maximum likelihood estimate. From the results, it can be shown that Kaplan Meier for both LS and ML has the least value of Anderson-Darling statistics which signifies the best-of-fit for porous ceramic. Also from Table 2, the shape parameter (Weibull modulus) of the least square estimate is higher than that of the maximum likelihood for the Kaplan Meier estimate. The scale parameter (characteristic strength) of the least square estimate shows higher value than that of the maximum likelihood. The threshold strength which is the minimum strength below which the material will not fail of the least square estimate is lower than that of the maximum likelihood.

Table 2: Summary of shape parameter, scale parameter, threshold and Anderson-Darling statistics of three-parameter Weibull using different estimates least square.

Estimate		*m*	σ_o	σ_u	AD
Mean	ML	2.21	5.53	12.97	1.31
Rank	LS	2.83	6.92	11.70	1.40
Median	ML	2.21	5.53	12.97	0.98
Rank	LS	2.78	6.59	11.99	1.07
Hazen	ML	2.21	5.53	12.96	0.83
	LS	2.72	6.31	12.24	0.91
Kaplan	ML	2.21	5.53	12.97	0.59
Meier	LS	3.28	7.27	11.18	0.77

Figure 5 and Figure 6 show the probability plots of the four probability of failure (mean rank, median rank, Hazen rank and Kaplan Meier) for LS and ML respectively. Kaplan Meier (Figure 5d and Figure 6d) has the best of fit for both LS and ML estimate, , because all the data points are within the upper and lower bounds of the 95% confidence interval. ML chases the upper probability of failure thereby fit the points closer to the upper part of the center line while the LS chases the lowest points of the probability points. The higher value of Weibull modulus of the porous ceramic as compared to other materials (Table 3) can be attributed to the relatively uniform of distribution of pores, which gives the porous sample greater reliability, because material under load may break from a sharp flaw but not break from a pore of similar size [11]. Threshold values i.e., the flexural strength below which the material will not fail was lowest for porous ceramic as compared with strength reported by literatures in Table 3. Researchers have normally assumed the threshold of brittle materials such as ceramics and glasses to be zero, which resulted in two-parameter Weibull modulus [28]. Due to relative high flexural strength value of mullite [29], the threshold value cannot be ignored. The calculated threshold strength of the porous sintered clay shows it can withstand the pressure applied during micro, ultra and nanofiltration. The pressure range required for these filtration processes is in the range 10-1000kPa (0.01-1MPa).

Table 3: Three-parameter Weibull of some engineering materials together with current research [21].

Materials	*m*	σ_u (MPa)
PMMA-based bone cement	0.5-1.4	-
Window glass	1.21	35.8
Silicon die	2-3	48-184
Ti-6Al-4V	2.6	563
Titanium Alloy 30NiCrMo16 steel	2.8	441
This research	2.21-3.28	11.18-12.97

Maximum likelihood value of the Weibull modulus is smaller than the least square estimate as shown in Table 2; ML values at 90 and 95% confidence interval are tighter than those from LS, hence statisticians and designers prefer ML [28].

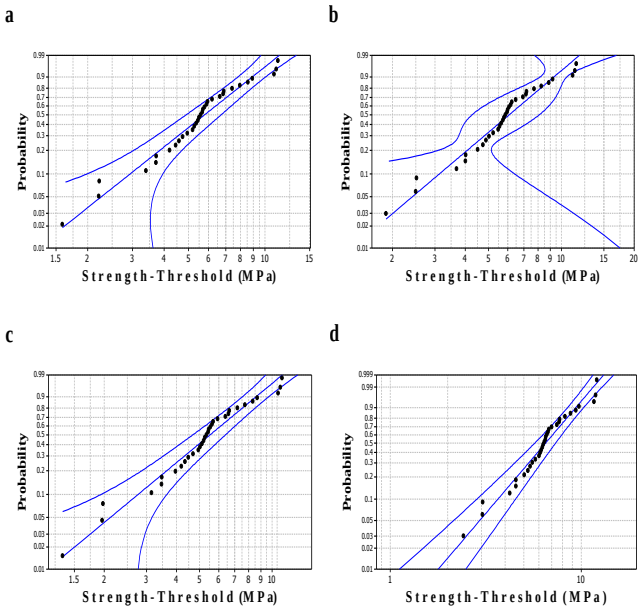

Figure 5: Probability plot (LS) for flexural strength (a) mean rank; (b) median rank; (c) Hazen rank; (d) Kaplan Meier

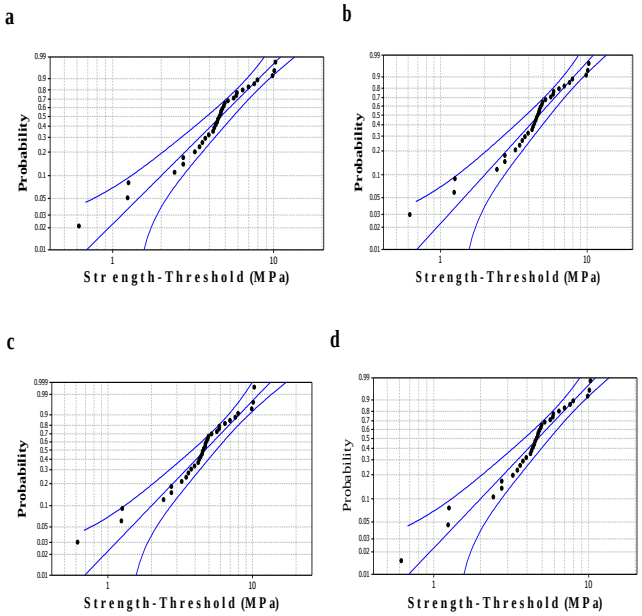

Figure 6: Probability plot (ML) for flexural strength (a) mean rank; (b) median rank; (c) Hazen rank; (d) Kaplan Meier

The summary of two parameter Weibull probability distribution of the porous sintered clay in Table 4 shows the Weibull modulus, scale parameter and Anderson Darling statistics of the different probability of failure estimates. Like the three parameter Weibull, Kaplan Meier estimates has the least value of Anderson Darling statistics, which signifies the best fit to model the reliability of the flexural strength. The scale parameter and the Weibull modulus of the two parameter Weibull probability distribution are higher than the Weibull modulus and threshold strength of the three-parameter Weibull probability distribution. Two-

parameter Weibull gives the failure at 63.2% of the tested materials while the three-parameter Weibull considers failure for all the tested materials. The three-parameter Weibull is the suitable tool to model the reliability of failure of brittle materials since it considers all the tested materials. LS is the simpler means of estimating the Weibull parameters by ranking the strength data from lowest to highest and assigning a probability estimator for the probability of failure. Maximum likelihood value of the Weibull modulus is smaller than the least square estimate as shown in Table 3; ML values at 90 and 95% confidence interval are tighter than those from LS, hence statisticians and designers prefer ML [11]. ML estimates the Weibull parameters by maximizing the Weibull likelihood function i.e., by iterating the Weibull parameters until the optimum parameters are obtained to fit the test data, which tends to converge the parameters to the same value irrespective of the failure probability estimate in Table 4.

Table 4 : Summary of shape parameter, scale parameter, threshold and Anderson-Darling statistics of two-parameter Weibull using different estimates least square.

Estimate		*m*	σ_o	AD
Mean	ML	7.58	18.92	1.31
Rank	LS	9.22	6.92	1.40
Median	ML	7.58	18.92	0.98
Rank	LS	9.75	6.59	1.07
Hazen	ML	7.58	18.92	0.83
	LS	10.22	6.31	0.91
Kaplan	ML	7.58	18.92	0.59
Meier	LS	9.52	7.27	0.77

The probability density function for the porous ceramic for least square (LS) and maximum likelihood (LS) are shown in Figure 7. The probability density function of ML is tighter than that of LS. This shows that LS estimate give higher failure probability than ML which gives more conservative failure probability. Both LS and ML probability density plots skewed to the left, this shows that the high probability of failure is toward the threshold strength. Figure 7 depicts that the porous ceramic has high uniformity, low variability and failure are highly predictable compared to other materials [21]. The width of the probability distribution is defined by the Weibull modulus. If the value of the Weibull modulus is large, the distribution will be narrow with a small spread of flexural strength. However, if value of Weibull modulus is small, the spread of the flexural strength is wide which signifies large variation. Based on the Weibull modulus obtained, the porous ceramic has relative higher reliability.

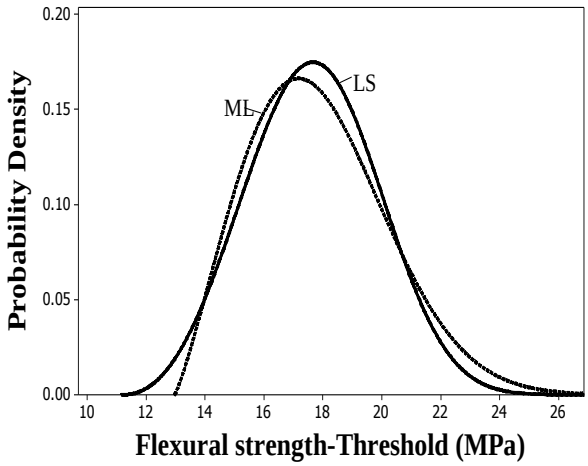

Figure 7: Probability density plot of LS and ML estimates.

Figure 8 shows the morphology of the fractured surface of the porous ceramic. The morphology of the porous ceramic shows a relative distribution of slit-shaped pores which resulted in high value of the Weibull modulus. The porous ceramic shows a relative distribution of slit-shaped pores as shown by BJH analysis. It is well known that a material under load may break under a sharp crack but not break from a blunt flaw such as pore of similar size and each type of flaw has its own distribution as reported by [11]. The presence of uniformly distributed pores in the sample makes the reliability of the porous material to be very high and of predictable failure strength.

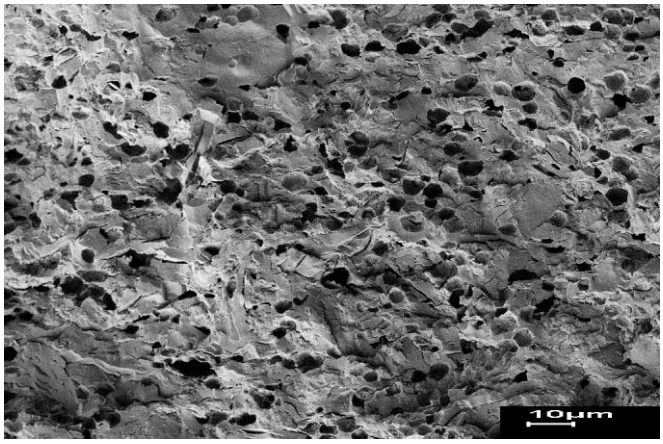

Figure 8: Fractured surface morphology of porous sintered clay.

4.0 CONCLUSION

The result of the XRD and XRF show that the clay is a good source of mullite ceramic which formed at temperature above 1100°C. The BET result shows that the porous sintered clay is mesoporous. Three-parameter Weibull can be used to model the variability and reliability of porous sintered clay. Kaplan Meier estimate give the best fit for the porous

sinterd clay due to the low value of Anderson-Darling statistics. Maximum likelihood estimate gives the overall best fit as compared to least square estimates. However, the Weibull modulus of the porous ceramic is relative higher, hence makes higher chances for the prediction of probability of failure. The morphology of the fractured surface of the porous ceramic shows relatively distribution of rounded pores which result in the high value of the Weibull modulus, high reliability and highly predictable. The three parameter Weibull shows that the porous sintered clay is suitable for membrane process in micro and ultrafiltration applications. Further research should be conducted for wastewater treatment to ascertain the filtration performance of the produced porous sintered clay.

ACKNOWLEDGEMENT

This research was sponsored by Universiti Teknologi Malaysia (RUG-4C044 and MG-00M51). Special thanks go to Ministry of Education Malaysia (MOE) through research grant FRGS 04H74 and Bayero University Kano through Tertiary Education Training Fund (TETFund) for sponsoring the PhD programme.

REFERENCES

1. She J. H. and Ohji T. 2002. Porous mullite ceramics with high strength," *Journal of Materials Science Letters* 21, 1833–1834.
2. Bai J. 2010. Fabrication and properties of porous mullite ceramics from calcined carbonaceous kaolin and α-Al2O3," *Ceramics International* 36, 673–678.
3. Fan X., E. D. Case, F. Ren, Y. Shu, and Baumann M. J. 2012. Part I: porosity dependence of the Weibull modulus for hydroxyapatite and other brittle materials.," *Journal of the mechanical behavior of biomedical material* 8, 21–36.
4. Sahnoun R. D. and Baklouti S. 2013. Characterization of flat ceramic membrane supports prepared with kaolin-phosphoric acid-starch," *Applied Clay Science* 83–84, 399–404.
5. Liu Y. F., X.-Q. Liu, H. Wei, and Meng G.Y. 2001. Porous mullite ceramics from national clay produced by gelcasting," *Ceramics International*, 27, 1–7.
6. Emani S., R. Uppaluri, and Purkait M. K. 2014. Microfiltration of oil–water emulsions using low cost ceramic membranes prepared with the uniaxial dry compaction method," *Ceramics International*, 40, 1155–1164.
7. Bouzerara F., a. Harabi, S. Achour, andLarbot A. 2006. Porous ceramic supports for membranes prepared from kaolin and doloma mixtures," *Journal of the European Ceramic Society*, 26, 1663–1671.
8. Jana S., M. K. Purkait, and Mohanty K. 2010. Preparation and characterization of low-cost ceramic microfiltration membranes for the removal of chromate from aqueous solutions," *Applied Clay Science*, 47, 317–324.
9. Nandi B. K., R. Uppaluri, and Purkait M. K. 2008. Preparation and characterization of low cost ceramic membranes for micro-filtration applications," *Applied Clay Science*, 42, 102–110.
10. Ghosh D., M. K. Sinha, and Purkait M. K. 2013. A comparative analysis of low-cost ceramic membrane preparation for effective fluoride removal using hybrid technique," *Desalination*, 327, 2–13.

11. Quinn J. B. and Quinn G. D., 2010. A practical and systematic review of Weibull statistics for reporting strengths of dental materials.," *Dental materials : official publication of the Academy of Dental Materials*, 26, 135–47.
12. Emani S., R. Uppaluri, and Purkait M. K. 2013. Preparation and characterization of low cost ceramic membranes for mosambi juice clarification," *Desalination*, 317, 32–40.
13. Vasanth D., G. Pugazhenthi, and Uppaluri R. 2011. Fabrication and properties of low cost ceramic microfiltration membranes for separation of oil and bacteria from its solution," *Journal of Membrane Science*, 379, 154–163.
14. Nandi B. K., B. Das, R. Uppaluri, and Purkait M. K. 2009. Microfiltration of mosambi juice using low cost ceramic membrane," *Journal of Food Engineering*, 95, 597–605.
15. Khemakhem S., R. Ben Amar, and Larbot A. 2007. Synthesis and characterization of a new inorganic ultrafiltration membrane composed entirely of Tunisian natural illite clay," *Desalination*, 206, 210–214.
16. Nandi B. K., R. Uppaluri, and Purkait M. K. 2008. Preparation and characterization of low cost ceramic membranes for micro-filtration applications," *Applied Clay Science*, 42, 102–110.
17. Yakub I., J. Du, and Soboyejo W. O. 2012. Mechanical properties, modeling and design of porous clay ceramics," *Materials Science and Engineering: A*, 558, 21–29.
18. Hsiung C. H. H., A. J. Pyzik, F. De Carlo, X. Xiao, S. R. Stock, and Faber K. T. 2013. Microstructure and mechanical properties of acicular mullite," *Journal of the European Ceramic Society*, 33, 503–513.
19. M. Abubakar, a. B. Aliyu, and Ahmad N. 2014. Characterization of Nigerian Clay as Porous Ceramic Material," *Advanced Materials Research*, 845, 256–260.
20. Hoshide T. and Okawa M. 2003. A Numerical Analysis of Ceramics Strength Affected by Material Microstructure," 12, 183–189.
21. Han Z., L. C. Tang, J. Xu, and Li Y. 2009. A three-parameter Weibull statistical analysis of the strength variation of bulk metallic glasses," *Scripta Materialia*, 61, 923–926.
22. Preda V., E. Panaitescu, A. Constantinescu, and Sudradjat S. 2010. Estimations and predictions using record statistics from the modified Weibull model, *WSEAS Transactions on Mathematics*, 427-437
23. Preda V., E. Panaitescu, A. 2010. Constantinescu, Bayes estimators of Modified-Weibull distribution parameters using Lindley's approximation, *WSEAS Transactions on Mathematics*, 539-549.
24. Abubakar M., A. B. Aliyu, and N. Ahmad. 2015. Flexural Strength Analysis of Dense and Porous Sintered Clay Using Weibull Probability Distribution, 761, 347–351.
25. Niola V., R. Oliviero, and Quaremba G.2005. The application of wavelet transform for estimating the shape parameter of a Weibull pdf, WSEAS International Conference. on Dynamical Systems and Control. 126-130.
26. Castelein O., B. Soulestin, J. P. Bonnet, and Blanchart P. 2001. The infuence of heating rate on the thermal behaviour and mullite formation from a kaolin raw material," 27, 0–5.
27. Li S., J. Zheng, W. Yang, and Zhao Y. 2007. A new synthesis process and characterization of three-dimensionally ordered macroporous ZrO2," *Materials Letters*, 61,4784–4786.
28. Stawarczyk B., M. Ozcan, A. Trottmann, C. H. F. Hämmerle, and Roos M. 2012. Evaluation of flexural strength of hipped and presintered zirconia using different

estimation methods of Weibull statistics.," *Journal of the mechanical behavior of biomedical materials*, 10, 227–34.

29. Schneider H., J. Schreuer, and Hildmann B. 2008. Structure and properties of mullite—A review," *Journal of the European Ceramic Society*, 28, 329–344.